RSC Advances

ROYAL SOCIETY OF CHEMISTRY

www.rsc.org/advances

Journal Name

ARTICLE

Adsorption of Congo red from water with spindle-like boehmite: The role of lattice plane (020)

Received 00th January 20xx,
Accepted 00th January 20xx

DOI: 10.1039/x0xx00000x

www.rsc.org/

Guangci Li,[a,*] Yuanyuan Sun, Xuebing Li,[a,*] and Yunqi Liu[b]

Spindle-like boehmites with high adsorption capacity for Congo red (CR) from water were prepared via a hydrothermal synthesis method without any surfactants. The crystallite sizes of boehmites can be subtly adjusted by hydrothermal post-treatment for various durations, and the crystalline structure, morphology and textural property of boehmites were characterized by different techniques. The adsorption capacities and rates of CR onto boehmites were thoroughly evaluated with the help of equilibrium and kinetics experiments. The adsorption isotherms are fitted well to the Langmuir equation, and the Langmuir adsorption capacity (q_{max}) is as high as 427.4 mg/g. The kinetics data show that the adsorption process can be well described by pseudo-second-order kinetics model, and besides, adsorption rate is closely related to the exposed surface area of lattice plane (020) of boehmite crystallite, because this plane has a relatively high OH density that is favorable to the adsorption of CR. The IR characterization and the relationship between the pH values of the zero point of charge (pH_{zpc}) for different boehmites and adsorption behavior of CR suggest that the involved adsorption process is driven by the hydrogen bonding and electrostatic attraction at the same time.

1. Introduction

Congo red (CR) (sodium salt of benzidinediazobis-1-naphthylamine-4-sulfonic acid), is one of the most used dyes in textile industry, giving wool and silk red colour with yellow fluorescence.[1] When CR exposes to air, it could be metabolized to benzidine that is known as a carcinogen and can cause some allergic responses.[2] Moreover, CR discharged into water resources is potential hazard to healthy, environment, and ecology. Thus, the CR-containing effluents have to be treated before they are discharged into environment. Recently, several techniques have been developed and implemented for the removal of CR molecules from dye effluents, such as adsorption, chemical oxidation, photo degradation, electrochemical process, and biodegradation.[3-10] The aromatics structure of CR, however, is very physicochemical, thermal and optical stabile, against photo or biodegradation,[11] and thus, adsorption by organic or inorganic adsorbents is becoming the most popular technique owing to high efficiency and simplicity.[12]

Many efforts have been paid to find various materials for the removal of CR molecules, including red mud, kaolin, fly ash, leaf powder, montmorillonite, hectorite, and the activated carbon from agricultural wastes.[13-19] Because most of them do not have sufficient adsorption capacities (less than 100 mg/g) towards CR molecules, several novel alternative adsorbents with relatively high adsorptive abilities are developed in recent years, as shown in Table 1.[20-28] Despite this, the involved synthesis methods and conditions are generally complicated and severe, which strongly limit their applications in practical field. Therefore, the development of facile methods to synthesize effective adsorbents is demanded to remove pollutants from water in large-scale.

Table 1. Comparison of adsorption capacity of CR onto various adsorbents.

Adsorbents	Adsorption capacity (mg/g)	References
MgO nanoplates	303.0	20
CTAB modified chitosan beads	352.5	21
Maghemite nanoparticles	208.3	22
Hierarchical NiO nanosheets	151.7	23
γ-Al_2O_3 nanoplates	176.7	24
Bentonite	158.7	25
$CoFe_2O_4$	244.5	26
PPy-PANI nanofibres	222.2	27
Hydroxyapatite-chitosan	769	28

Boehmite (γ-AlOOH), an alumina hydrate, can be easily prepared by acid-base precipitation method, sol-gel method and hydrothermal method,[29-31] and its high surface area and large volume are favourable to the adsorption and diffusion of bulky molecules. Furthermore, the pH value of the zero point of charge (pH_{zpc}) of boehmite is 9.7,[32] which is suitable for the adsorption of anionic dyes because of favourable electrostatic attraction. Currently, several studies have confirmed the feasibility of boehmite used as

[a] Key Laboratory of Biofuels, Qingdao Institute of Bioenergy and Bioprocess Technology, Chinese Academy of Sciences, Qingdao, 266101, P. R. China. E-mail address: ligc@qibebt.ac.cn (G. Li), lixb@qibebt.ac.cn (X. Li).
[b] State Key Laboratory of Heavy Oil Processing, Key Laboratory of Catalysis, CNPC, China University of Petroleum, Qingdao, 266555, PR China.
†Electronic Supplementary Information (ESI) available. See DOI: 10.1039/x0xx00000x

adsorbent to remove CR. For instance, Zhang et al. prepared boehmite materials with core/shell structures and investigated their adsorption capacities toward CR.[33] They thought that superior adsorption abilities are ascribed to the hollow microstructure and high specific surface area of boehmite. Cai et al. compared different aluminium hydroxide samples with hollow sphere structure for CR adsorption, and found that the crystallinity of boehmite markedly influences its adsorption performance, and besides, all boehmite samples have better adsorption capacities than the amorphous samples.[34] Although the relationship between the crystallinity of boehmite and its adsorption capability has been known, the effects of crystallinite size and various lattice planes are still not clear. It is generally agreed that the surface OH groups of boehmite play a key role in adsorption process, and the number and distribution of OH groups strongly depend on the exposed lattice planes.[30] Thus, understanding the relationship between the lattice plane of boehmite and the adsorption behaviour, capacity and rate, is important for developing boehmite materials with potential industrial application.

In this contribution, spindle-like boehmite is synthesized through a simple hydrothermal process, and then is employed to remove CR from aqueous solution. In order to investigate the effect of crystallite size on CR adsorption, a series of boehmites with various crystallite sizes are prepared through a hydrothermal post-treatment of the as-prepared boehmite for different durations. We found that boehmite with higher pH_{zpc} value exhibits a higher adsorption capacity towards CR, and increasing the crystallite size along the lattice plane (020) of boehmite can accelerate the adsorption of CR onto boehmite surface.

2. Experimental

2.1. Preparation of boehmite materials

All reagents of analytical grade are purchased from Sinopharm Chemical Reagent Co., Ltd., and are used without further purification. Typically, 2.50 g of $AlCl_3 \cdot 6H_2O$ was dissolved into 25 ml of deionized water under magnetic stirring at room temperature. Then, 25 ml of dimethylformamide (DMF) was added into the above solution. Afterward, the resulting homogeneous mixture was transferred into a 100 ml Teflon-lined stainless autoclave, kept at 160 °C for 3 h, and then cooled down naturally. The precipitate was collected by centrifugation, washed with deionized water for several times until no Cl^- ions were detected by $AgNO_3$, and then dried at 120 °C overnight. The obtained sample was labelled as B-0.

Other samples were obtained by further hydrothermal treatment of B-0. Typically, 5.0 g of B-0 was suspended in 50 ml deionized water, and then transferred into a 100 ml Teflon-lined stainless autoclave. The mixture was treated at 140 °C for 4, 8, 12, 16, 20 h, respectively, and the obtained samples were labelled correspondingly as B-4, B-8, B-12, B-16, and B-20.

2.2. Characterization

The X-ray powder diffraction (XRD) patterns of the samples were recorded by a Bruker D8 ADVANCE diffractometer, using Cu Kα radiation (λ = 1.5406 Å) at a scan rate (2ϑ) of 2° min^{-1}. The accelerating voltage and applied current are 40 kV and 40 mA, respectively. The crystallite size of samples was calculated by means of the Scherrer formula ($D = 0.89\lambda/\beta\cos\vartheta$, where D, λ, β, and ϑ are crystallite size, wavelength (1.5406 Å), full width at half-maximum intensity (FWHM) of diffraction peaks in radians, and Bragg's diffraction angle, respectively).

The morphologies and microstructures of the as-prepared samples were observed by field emission scanning electron microscopy (FE-SEM, Hitachi S-4800) and transmission electron microscopy (TEM, JEOL JEM-2100UHR).

The specific surface areas and pore size distributions were determined from nitrogen adsorption-desorption isotherms measured on a Micromeritics TRISTAR 3020 adsorption analyser at -196 °C. All of the samples were degassed at 140 °C in vacuum for 8 h prior to adsorption measurements. The pH value of the zero point of charge (pH_{zpc}) was determined by titration method as reported previously.[35]

The spectral shapes of the samples were identified by Fourier transform infrared spectroscopy (FT-IR, Newus Nicolet) at room temperature using KBr disks.

2.3. Adsorption equilibrium and kinetics measurements

Adsorption isotherms were obtained by treating CR solutions with different concentrations. Briefly, 30 mg of boehmite samples was added to 100 ml conical flasks containing 40 ml of CR solutions with the concentration ranging from 150 to 330 mg/L. The conical flasks were then sealed and transferred into a shaker, followed by shaking for 24 h to reach adsorption equilibrium. The amount of CR at equilibrium on the adsorbent samples, q_e (mg/g), was calculated by the following equation:

$$q_e = \frac{(C_0 - C_e) \times V}{m} \quad (1)$$

where C_0 and C_e (mg/L) are the concentrations of CR solution at initial and equilibrium, respectively, V (L) is the volume of the solution and m (g) is the mass of adsorbent used.

To investigate the adsorption kinetics of CR, similar experiments to those of equilibrium experiments were carried out. Typically, 30 mg of absorbent samples was added to a series of beakers filled with 40 ml of CR solution with a concentration of 170 mg/L under magnetic stirring. At several time intervals, a series of liquid samples were obtained. The amount of adsorption at time t, q_t (mg/g), was calculated according to the following equation:

$$q_t = \frac{(C_0 - C_t) \times V}{m} \quad (2)$$

where C_0 and C_t (mg/L) are the concentrations of CR solution at initial and any time t, respectively, V (L) is the volume of the solution and m (g) is the mass of adsorbent used. The concentrations of CR solutions were measured at λ_{max} = 498 nm by using Beckman DU800 UV/vis Spectrophotometer.

3. Results and discussion

3.1. Characterization of boehmite samples

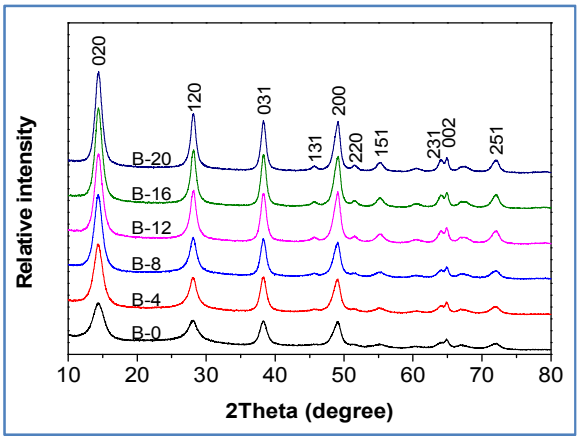

Figure 1. XRD patterns of the as-prepared boehmite samples.

Figure 1 shows the characterization of crystalline structure of the obtained samples, in which all diffraction peaks are in good agreement with those of the orthorhombic boehmite phase (JCPDS 00-21-1307). Apparently, with prolonging the hydrothermal duration, the shape of diffraction peaks becomes sharper and their intensities increase as well, indicating that their crystallite sizes become larger. Taking into account the assumption of a parallelepiped shape for boehmite crystallite, the characteristic diffraction peaks (020), (200), and (002) is directly correlated to the dimensions along the *b*, *c*, and *a* axes.[30] Thus, the corresponding crystallite sizes can be calculated by Scherrer equation according to the three basal planes, and the results are listed in Table 2. The sizes along the three directions for B-0 are smaller than that of the hydrothermal post-treated samples, suggesting that the as-obtained crystallites further grow under hydrothermal conditions, and the lattice plane perpendicular to the plane (002) grows more rapidly than the others. After the treatment for 12 h, the growth rate of the crystallites becomes mild. P. Raybaud et al. have used ab initio calculations and molecular dynamics to study water-boehmite interfacial properties, and they calculated that the surface energies of the basal plane (010), (100), and (001) are in order: 465, 650, and 750 mJ/m^2,[36] indicating that the plane (010) has the lowest surface energy and thus are preferentially formed from the view of thermodynamics. Because the plane (020) has the same orientation as the plane (010), the surface energy of the plane (020) is the lowest compared to that of other planes. Thus, the plane (020) has the largest surface area and its growth rate is more rapid in this work. Generally, as the crystallinity of boehmite becomes higher, the amounts of bonding water and surface OH groups decrease correspondingly. Because the surface charge of boehmite in water arises from surface OH groups, pH_{zpc} of the six samples reduced in lines with the duration (see Table 2), which will further affect their adsorption capacities in water.

Table 2. Properties of the as-prepared boehmites.

Sample		B-0	B-4	B-8	B-12	B-16	B-20
Specific surface area (m^2/g)		194	181	170	158	148	140
Pore volume (cm^3/g)		0.46	0.50	0.56	0.59	0.60	0.60
Pore diameter (nm)		9.8	12.2	12.4	12.9	13.7	14.3
Crystallite size (nm)	$D_{(020)}$	4.8	5.3	5.4	5.6	5.7	5.8
	$D_{(200)}$	6.7	6.9	7.1	7.6	7.8	8.1
	$D_{(002)}$	15.2	17.6	19.2	20.7	23.3	23.6
pH_{zpc}		9.1	8.8	8.4	8.0	7.9	7.7

The morphology and microstructure of the as-prepared samples were investigated by SEM and TEM, as shown in Figure 2 for B-0 sample. The low-magnification SEM and TEM images (Figure 2a and 2c) show that the obtained boehmite is composed of uniform spindle-like particles with 0.8-1.2 μm in length and 40-60 nm in width without other morphologies or agglomerates. The high-magnification SEM and TEM images (Figure 2b and 2d) reveal that the spindle-like structures are constructed of small nanoplates, and these nanoplates are consisted of smaller flake-like units with approximate size in a range of 10 to 30 nm in length, which is consistent with the crystalline sizes calculated from XRD patterns. All post-treated samples also have similar morphologies and structures (see Figure S1 in Supplementary data), indicating that hydrothermal post-treatment for longer duration does not change the morphology, but rather affects the size and surface properties of boehmite crystallites.

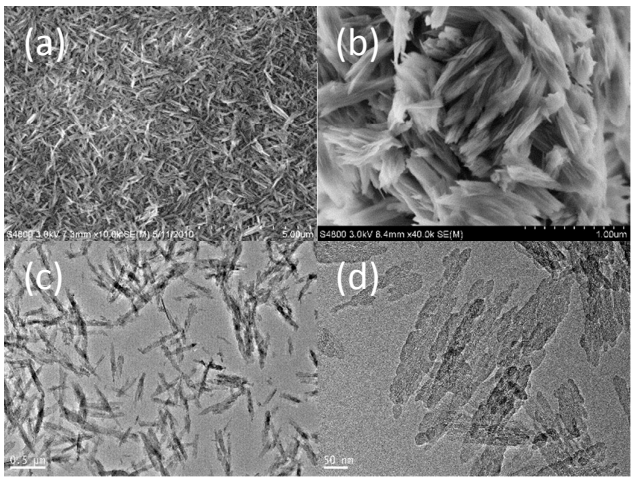

Figure 2. SEM images (a, b) and TEM image (c, d) of sample B-0.

The textural properties of the as-prepared samples were characterized via N_2 adsorption/desorption method (see Figure S2), and the specific surface area, pore volume, and average pore diameter of them are listed in Table 2. The isotherms for all samples are of type II, suggesting the presence of mesopores and macropores. In addition, the pore diameters of mesopores increase gradually from 9.8 to 14.3 nm with prolonging the hydrothermal duration, on the contrary, the specific surface areas of boehmite samples decrease because of the formation of larger secondary particles from primary crystallites aggregation and growth. The pore volumes thus increase corresponding to the crystallite size because the pores of boehmite mainly arise from the gaps between particles or aggregates. When the hydrothermal duration exceeds 16 h, however, pore volume does not increase more, since larger crystallites would occupy more spaces, leading to a relative reduction of pore volume.[37]

3.2. Adsorption of CR

3.2.1. Adsorption equilibrium

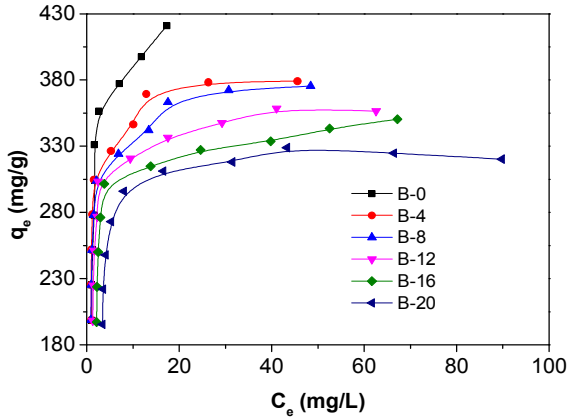

Figure 3. Adsorption isotherms for CR onto different boehmite samples at 25 °C. (adsorbent dose 750 mg/L, CR concentration 150-330 mg/L)

The adsorption isotherms for CR adsorption onto boehmite samples were obtained by treating CR solution with different initial concentrations at room temperature. As shown in Figure 3, the adsorption amount of CR increases sharply as the initial CR concentration increased up to 210 mg/L, leading to an equilibrium concentration lower than 10 mg/L. The adsorption amount increases slowly with CR initial concentration over 210 mg/L and then inclines to achieve saturation gradually. Despite the similar tread of adsorption isotherms, the adsorption capacities of the samples are far different.

The Freundlich and Langmuir isotherms, two common models for adsorption, were selected to fit the adsorption isotherms. The Freundlich equation can be expressed as follows:[38]

$$\log q_e = \log K_F + \frac{1}{n}\log C_e \qquad (3)$$

where q_e (mg/g) is the amount of CR adsorbed at equilibrium, C_e (mg/L) is the concentration of CR solution at equilibrium, K_F ($mg^{1-1/n}\cdot L^{1/n}/g$) and n are the Freundlich adsorption isotherm constants, respectively. The poor linear relationships between $\log C_e$ and $\log q_e$ (see Figure S3) and the low coefficient (R^2) values for all samples (see Table 3) suggest that Freundilch model are not suitable to describe CR adsorption process onto boehmite.

The Langmuir equation is based on the assumption of a structurally homogeneous adsorbent where all sorption sites are identical and energetically equivalent. The Langmuir equation is expressed as follows:[39]

$$\frac{C_e}{q_e} = \frac{1}{q_{max}K_L} + \frac{C_e}{q_{max}} \qquad (4)$$

where C_e (mg/L) is the equilibrium concentration of CR in solution, q_e (mg/g) is the equilibrium capacity of CR on the adsorbent, q_{max} (mg/g) is the maximum amount of CR on the adsorbent to form a complete monolayer on surface, K_L (L/mg) is the Langmuir constant that relates to the affinity of adsorption sites. As shown in Figure S4, all plots show linear relationship over the whole concentration ranges and the correlation coefficients (R^2) are higher than 0.99 (see Table 3), which imply that the adsorption of CR onto spindle-like boehmite fits well with the Langmuir model.

Table 3. Parameters of two adsorption models for the adsorption of CR onto boehmites.

Sample	Freundilch adsorption model			Langmuir adsorption model			
	n	K_F ($mg^{1-1/n}\cdot L^{1/n}/g$)	R^2	q_{max} (mg/g)	K_L (L/mg)	R^2	R_L ($\times 10^3$)
B-0	4.57	246.43	0.717	427.4	1.12	0.996	2.70
B-4	7.45	247.91	0.758	384.6	1.50	0.997	2.02
B-8	7.55	241.10	0.823	380.2	1.26	0.995	2.40
B-12	8.29	232.01	0.762	362.3	1.14	0.997	2.65
B-16	8.40	219.63	0.722	352.1	0.78	0.993	3.87
B-20	8.29	203.70	0.685	327.9	0.83	0.993	3.64

Additionally, adsorption amount of CR increases with pH_{zpc} of boehmite, as shown in Figure 4. This is because that the surface charge of boehmite is strongly dependent on the pH value of the aqueous solution, that is positive if pH (solution) < pH_{zpc}, or negative if pH (solution) > pH_{zpc}. The pH of CR solution used in this work is neutral, thus all samples have positive surface charge, which facilitates the adsorption of complex anion of CR. Boehmite with higher pH_{zpc} would possess more net surface charge that can supply more adsorption active sites for anions, and thus the adsorption capacity of samples increases linearly with pH_{zpc}.

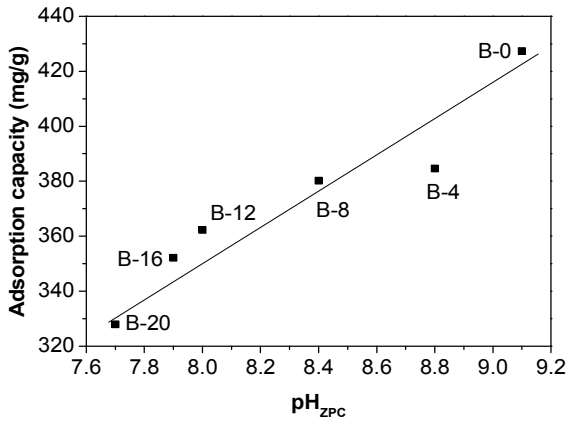

Figure 4. The relationship between pH_{zpc} value and adsorption capacity for all samples.

The favourability of an adsorption system under specific conditions can be predicated by the Langmuir isotherm shape. According to the study of Hall et al.,[40] the feature of Langmuir isotherm can be expressed in terms of a dimensionless constant, separation factor (R_L) that is defined by the following equation:

$$R_L = \frac{1}{1+K_L C_0} \qquad (5)$$

where C_0 (mg/L) is the highest initial solution concentration and K_L (L/mg) is the Langmuir constant. The values of R_L are basically classified into four types of the isotherm: (i) unfavourable ($R_L > 1$); (ii) linear ($R_L = 1$); (iii) favourable ($0 < R_L < 1$); (iv) irreversible ($R_L = 0$). Herein, the values of R_L are in the range of 0 to 1 (Table 3), suggesting that the adsorptions onto all samples are favourable in this work. It is worth to note that the values of R_L are very close to zero, which means that although the adsorption of CR onto

boehmite particles is a reversible process, its desorption process is difficult to take place under moderate conditions, and this interactions between anions of CR molecule and net positive charged boehmite surface are strong and stable.

Among these samples, the maximum adsorption capacity for the adsorption of CR onto spindle-like boehmite calculated by the Langmuir model (q_{max}) is as much as 427.4 mg/g, which is higher than most reported values for CR adsorption onto other adsorbents (see Table 1).

3.2.2. Adsorption kinetics

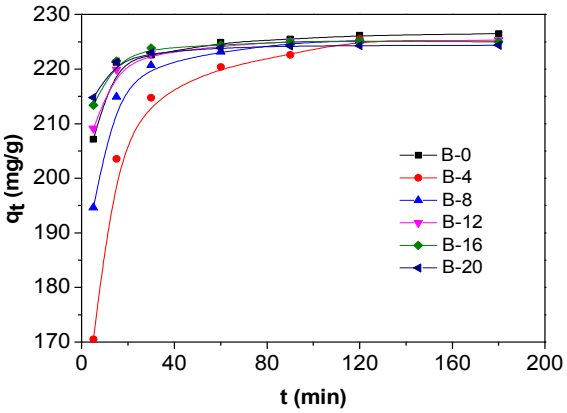

Figure 5. Adsorption kinetics of CR onto different samples at 25 °C. (adsorbent dose 750 mg/L, CR initial concentration 170 mg/L)

Figure 5 shows the adsorption amounts of CR onto different boehmites versus adsorption time with initial concentration of 170 mg/L. Apparently, the adsorption amount increases with prolonging the contact time, and CR is rapidly adsorbed in the initial 15 min, and then gradually achieves the equilibrium within 120 min for all samples. Although their adsorption processes and tendencies are similar, adsorption rates are much different according to the q_t values at the initial stage for different samples. For fitting the kinetics data and calculating adsorption rate, two common kinetics models, pseudo-first-order and pseudo-second-order were employed.

Table 4. Parameters of two kinetics models for the adsorption of CR onto boehmites.

Samples	Pseudo-first-order			Pseudo-second-order		
	q_e (mg/g)	$k_1 \cdot 10^2$ (min^{-1})	R^2	q_e (mg/g)	$k_2 \cdot 10^2$ (g/mg min^{-1})	R^2
B-0	11.1	2.15	0.868	227.3	0.88	0.999
B-4	29.2	1.97	0.798	227.3	0.25	0.998
B-8	15.1	1.92	0.830	226.8	0.53	0.999
B-12	7.41	2.13	0.805	225.7	1.12	0.999
B-16	4.53	1.56	0.595	225.7	1.53	0.998
B-20	4.09	1.98	0.773	224.7	1.92	0.999

Pseudo-first-order model, widely used for analyzing the adsorption in aqueous solution, can be expressed as follows:[41]

$$\log(q_e - q_t) = \log q_e - \frac{k_1}{2.303} t \quad (6)$$

where q_e (mg/g) and q_t (mg/g) are the amount of CR adsorbed at equilibrium and at time t (min), respectively. k_1 (1/min) is the equilibrium rate constant. As shown in Figure S5, however, the plots of log ($q_e - q_t$) versus t do not give linear relationships during the whole adsorption, and the calculated adsorption capacities of this model are much lower than the actual values in the experiments (see Table 4), suggesting that the pseudo-first-order model cannot describe the adsorption behaviour of CR in this work.

Pseudo-second-order model based on equilibrium adsorption can be expressed as follows:[42]

$$\frac{t}{q_t} = \frac{1}{k_2 q_e^2} + \frac{1}{q_e} t \quad (7)$$

where k_2 (g/mg min) is the equilibrium rate constant of pseudo-second-order equation. As shown in Figure S6 and Table 4, the plots of t/q_t versus t based on Equation (4) give good linear relation and the coefficient (R^2) values are greater than 0.99 for all samples, indicating that adsorption of CR onto boehmite here can be well described by the pseudo-second-order model.

Among the samples, B-20 is the first to achieve adsorption equilibrium, which may be related to its smaller specific surface area and lower adsorption amount. In contrast, B-4 is the last to achieve equilibrium because of the higher adsorption capacity. Combining with their pore sizes, it is thought that for the post-treated samples, larger pore size is favourable to the diffusion of CR molecules from external surface to internal surface, leading to adsorption equilibrium in a short time. Compared to the post-treated samples, however, B-0 has the highest adsorption capacity and smallest pore size, but its adsorption rate is not slowest. Therefore, textural property is not unique influence on the adsorption rate of CR.

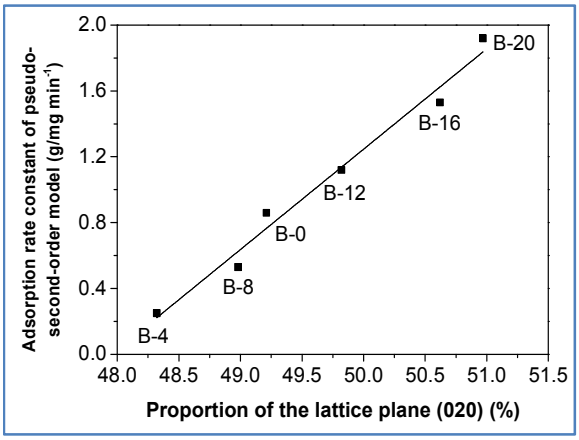

Figure 6. Relationship between surface area of plane (020) and adsorption rate for all samples.

For boehmite crystallite, comparing to the planes (200) and (002), the plane (020) is the basal face which possesses highest surface OH group density, and this plane exhibits the smallest interfacial energy and the highest development.[36] Therefore, the plane (020) represents major surface area and has most surface OH groups of boehmite, which will have a certain influence on adsorption

process. According to the data in Table 2, the surface area of the plane (020) for each sample can be calculated by using the size along *a* direction ($D_{(002)}$) to multiply the size along *c* direction ($D_{(200)}$), and the values are in order: B-0 (101.8 nm^2), B-4 (121.4 nm^2), B-8 (136.3 nm^2), B-12 (157.3 nm^2), B-16 (181.7 nm^2), B-20 (191.2 nm^2). Similarly, the surface areas of the planes (002) and (200) for different samples can also be calculated, and then the proportion of the three surface will be obtained by dividing each surface area by the total area. It is found that there is a good relationship between the proportion of the lattice plane (020) and the adsorption rate (see Figure 6). In view of this, it is believed that as the basal plane, plane (020) plays a key role in CR adsorption. As the hydrothermal post-treatment time is prolonged, the surface area of the plane (020) grows gradually, resulting in more surface OH groups. In addition, the specific surface area of boehmites decreases with the growth of crystallite, leading to an increase in the surface OH group numbers per area correspondingly. Thus, CR anions may interact with these OH groups by hydrogen bonds, and high surface OH group density promotes the rapid adsorption of CR in a short time.

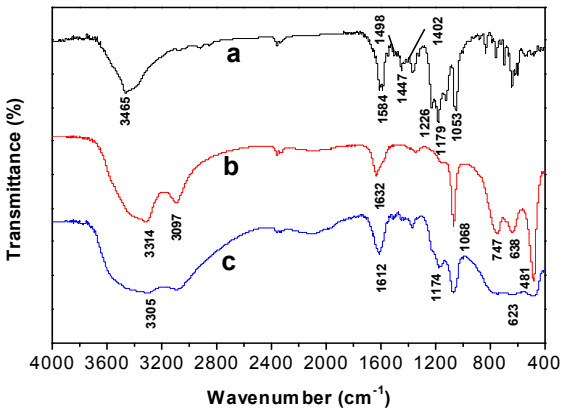

Figure 7. FTIR spectra of CR (a), B-0 before (b) and after (c) adsorption.

In order to determine which groups are responsible for adsorption, the surface groups of the adsorbate and adsorbent are detected by means of FTIR technique. As shown in Figure 7, many changes in band positions of IR spectra for CR and B-0 are found after adsorption. With respect to CR spectrum, the bands at 3465 and 1584 cm^{-1} assigned to stretching vibration of –N–H and –N=N– respectively diminish after adsorption, meanwhile, the bands at 1226, 1179, and 1053 cm^{-1} corresponding to S=O stretching vibrations diminish as well. And also, the band at 1179 cm^{-1} shifts to a low wavenumber of 1174 cm^{-1}. These changes indicate that the –N–H, –N=N– and $–SO_3$ groups of CR are involved in the adsorption process. In addition, the bands at 1498, 1447, 1402 cm^{-1} assigned to aromatic skeletal vibrations have been shifted, broadened, and reduced after adsorption. With respect to B-0, the bands at 3314 and 3097 cm^{-1} assigned to (Al)O–H stretching vibrations diminish after adsorption, and the band at 3314 cm^{-1} broadens and shifts to a low wavenumber of 3305 cm^{-1}. The band at 1632 cm^{-1} attributed to the –OH bending vibration of H_2O of boehmite strengthens and shifts to a low wavenumber of 1612 cm^{-1}. The band at 1068 cm^{-1} assigned to Al–O–H bending vibration is also reduced. Moreover, the bands at 747, 638 and 481 cm^{-1} corresponding to the vibration mode of AlO_6 are still observed but diminish to a certain extent, and the band at 638 cm^{-1} shifts to a low wavenumber of 623 cm^{-1} as well. The IR analysis results reveal that there are strong interactions between the surface of boehmite and some groups of CR, which affect simultaneously the vibrations of chemical bonds of boehmite and CR.

Considering that there are large amounts of hydroxyl groups locating on the surface of boehmite, it is reasonable to believe that these hydroxyl groups formed hydrogen bonds with some of elemental compositions of CR, such as N, S, O, and benzene ring during adsorption process. Besides, due to high pH_{zpc} as mentioned above, the boehmite surface is positively changed, and adsorption of anionic CR can take place easily because of the electrostatic attraction. Therefore, both hydrogen bonds and electrostatic attraction play key roles in the adsorption of CR onto boehmite surface. This is the reason why the adsorption amount of B-20 is the lowest, while its adsorption rate is the highest.

3.2.3. Thermodynamics studies

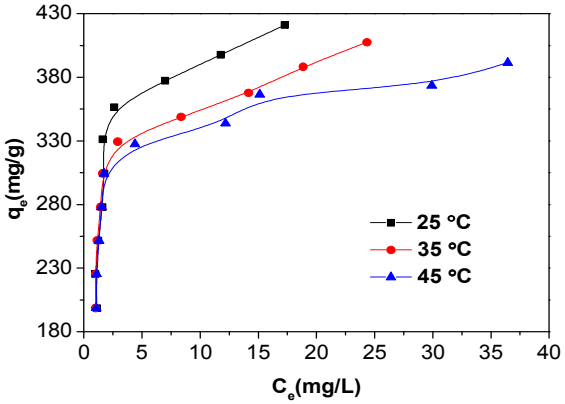

Figure 8. Adsorption isotherms for CR onto B-0 at different temperatures. (adsorbent dose 750 mg/L, CR concentration 150-330 mg/L)

Due to the high adsorption capacity, B-0 was selected to treat CR solutions with different initial concentrations at different temperatures to investigate the thermodynamics parameters of the adsorption of CR, and its adsorption isotherms are shown in Figure 8. The adsorption capacity of B-0 decreases as the temperature is increased, and the adsorption equilibrium achieves more rapidly at relatively high temperature, which means that high temperature is unfavourable to CR adsorption. As seen from Table 5, the adsorption capacity decreases slightly when the temperature is increased from 25 to 45 °C, suggesting that the adsorption process is an exothermic process.

The thermodynamics parameters, such as the Gibbs free energy (ΔG^0), the enthalpy (ΔH^0) and the entropy (ΔS^0), are calculated by using equilibrium constants at different temperatures. When the adsorption reaches the equilibrium state, ΔG^0 can also be calculated by the following equation (8):

$$\Delta G^0 = \Delta H^0 - T\Delta S^0 \quad (8)$$

$$\ln K = -\frac{1}{RT}\Delta H^0 + \frac{1}{R}\Delta S^0 \quad (9)$$

Thus, ln*K* can be expressed in Eq. (9), and the changes in the standard enthalpy and entropy of the adsorption can be estimated from the slope and intercept for a liner plot of ln*K* versus 1/*T* (see Figure S7). The thermodynamics parameters at different

temperatures for the initial CR concentration of 330 mg/L are listed in Table 5. The changes in ΔG^0 during the adsorption process are all negative, indicating that the adsorption process is spontaneous. The values of ΔG^0 in this study are between -20 and 0 kJ/mol, which suggests that this process is controlled by physical adsorption.[43] The negative value of ΔH^0 also indicates the exothermic nature of the adsorption. Moreover, the negative value of ΔS^0 shows that the adsorbed CR molecules on the surface of boehmite are organized in a more ordered fashion compared to those in solution.

Table 5. Thermodynamics parameters for the adsorption of CR onto B-0 at different temperatures.

Sample	q_{max} (mg/g)	Temperature (K)	ΔG^0 (kJ/mol)	ΔH^0 (kJ/mol)	ΔS^0 (J/mol K)
B-0	427.4	298	-7.306	-31.580	-81.457
	409.8	308	-6.491		
	392.2	318	-5.677		

4. Conclusions

Hierarchical boehmite materials with spindle-like morphology are prepared by a facile template-free hydrothermal process. The spindle-like boehmite particles are consisted of several smaller nanoplates. The hydrothermal post-treatment has a great effect on the properties of product, which leads to the growth of boehmite crystallites and the reduction of their surface areas. The adsorption of CR onto boehmite can be well described and explained by Langmuir adsorption isotherm and pseudo-second-order kinetics model. The analysis results indicate that the surface area of the lattice plane (020) of boehmite affects directly the adsorption rate, while the adsorption capacity is controlled by surface charge that depends on pH_{zpc} of boehmite. Moreover, FTIR analysis indicates that between CR molecule and boehmite surface, there are strong interactions that are attributed to the hydrogen bonds and electrostatic attraction. The thermodynamics parameters confirm that the adsorption of CR onto boehmite is a spontaneous physical process with an exothermic behavior. Since the as-prepared boehmite has a high adsorption capacity (427.4 mg/g), and the adsorption process can achieve equilibrium rapidly (within 120 min), it can be used as an effective adsorbent for removing Congo red from wastewater in the future.

Acknowledgements

Financial supports from the China Postdoctoral Science Foundation (No. 2015M572093) are gratefully acknowledged.

References

1 E. Lorenc-Grabowska and G. Gryglewicz, Dyes Pigments 2007, 74, 34.
2 I.D. Mall, V.C. Srivastava, N.K. Agarwal and I.M. Mishra, Chemosphere 2005, 61, 492.
3 C. Namasivayam and D. Kavitha, Dyes Pigments 2002, 54, 47.
4 R. Ahmad and R. Kumar, Appl. Surf. Sci. 2010, 257, 1628.
5 G. Sun and X. Xu, Ind. Eng. Chem. Res. 1997, 36, 808.
6 P. Gharbani, S.M. Tabatabaii and A. Mehrized, Int. J. Environ. Sci. Technol. 2008, 5, 495.
7 M. Khadhraoui, H. Trabelsi, M. Ksibi, S. Bouguerra and B. Elleuch, J. Hazard. Mater. 2009, 161, 974.
8 R.K. Wahi, W. Yu, Y. Liu, M.L. Mejia, J.C. Falkner, W. Nolte, and V.L. Colvin, J. Mol. Catal. A – Chem. 2005, 242, 48.
9 M.F. Elahmadi, N. Bensalah and A. Gadri, J. Hazard. Mater. 2009, 168, 1163.
10 K.P. Gopinath, S. Murugesan, J. Abraham and K. Muthukumar, Bioresource Technol. 2009, 100, 6295.
11 R. Han, D. Ding, Y. Xu, W. Zou, Y. Wang, Y. Li and L. Zou, Bioresource Technol. 2008, 99, 2938.
12 H.S. Rai, M.S. Bhattacharyya, J. Singh, T.K. Bansal, P. Vats and U.C. Banerjee, Crit. Rev. Sci. Technol. 2005, 35, 219.
13 C. Namasivayam and D.J.S.E. Arasi, Chemosphere 1997, 34, 401.
14 V. Vimonses, S. Lei, B. Jin, C.W.K. Chow and C. Saint, Chem. Eng. J. 2009, 148, 354.
15 B. Acemioğlu, J. Colloid Interf. Sci. 2004, 274, 371.
16 K.G. Bhattacharyya and A. Sarma, Dyes Pigments 2003, 57, 211.
17 L. Wang and A. Wang, J. Hazard. Mater. 2008, 160, 173.
18 C. Xia, Y. Jing, Y. Jia, D. Yue, J. Ma and X. Yin, Desalination 2011, 265, 81.
19 K. Nagarethinam and M. Mariappan, Water Air Soil Pollut. 2002, 138, 289.
20 J. Hu, Z. Song, L. Chen, H. Yang, J. Li and R. Richards, J. Chem. Eng. Data 2010, 55, 3742.
21 S. Chatterjee, D.S. Lee, M.W. Lee and S.H. Woo, Bioresource Technol. 2009, 100, 2803.
22 A. Afkhami and R. Moosavi, J. Hazard. Mater. 2010, 174, 398.
23 B. Cheng, Y. Le, W. Cai and J. Yu, J. Hazard. Mater. 2011, 185, 889.
24 W. Cai, J. Yu and M. Jaroniec, J. Mater. Chem. 2010, 20, 4587.
25 E. Bulut, M. Ozacar and I.A. Sengil, J. Hazard. Mater. 2008, 154, 613.
26 L. Wang, J. Li, Y. Wang, L. Zhao and Q. Jiang, Chem. Eng. J. 2012, 181-182, 72.
27 M. Bhaumik, R. McCrindle and A. Maity, Chem. Eng. J. 2013, 228, 506.
28 H. Hou, R. Zhou, P. Wu and L. Wu, Chem. Eng. J. 2012, 211-212, 336.
29 K. Okada, T. Nagashima, Y. Kameshima, A. Yasumori and T. Tsukada, J. Colloid Interf. Sci. 2002, 253, 308.
30 M. Nguefack, A.F. Popa, S. Rossignol and C. Kappenstein, Phys. Chem. Chem. Phys. 2003, 5, 4279.
31 T. He, L. Xiang and S. Zhu, Langmuir 2008, 24, 8284.
32 H.S. Potdar, K.W. Jun, J.W. Bae, S.M. Kim and Y.J. Lee, Appl. Catal. A-Gen. 2007, 321, 109.
33 L. Zhang, W. Lu, L. Yan, Y. Feng, X. Bao, J. Ni, X. Shang and Y. Lv, Micropor. Mesopor. Mater. 2009, 119, 208.
34 W. Cai, J. Yu, B. Cheng, B. Sun and M. Jaroniec, J. Phys. Chem. C 2009, 113, 14739.
35 Y. Wang, C. Bryan, H. Xu, P. Pohl, Y. Yang and C.J. Brinker, J. Colloid Interface Sci. 2002, 254, 23.
36 P. Raybaud, M. Digne, R. Iftimie, W. Wellens, P Euzen and H. Toulhoat, J. Catal. 2001, 201, 236.
37 J. Sánchez-Valente, X. Bokhimi and F. Hernández, Langmuir 2003, 19, 3583.
38 H.M.F. Freundlich, Z. Phys. Chem. 1906, 57, 385.
39 I. Langmuir, J. Am. Chem. Soc. 1918, 40, 1361.
40 K.R. Hall, L.C. Eagleton, A. Acrivos and T. Vermeulen, Ind. Eng. Chem. Fundam. 1966, 5, 212.
41 S. Lagergren, Kungliga Svenska Vetenskapsakademiens, Handlingar 1898, 24, 1-39.
42 Y.S. Ho and G. McKay, Process Biochem. 1999, 34, 451.

43 Y. Yu, Y. Zhuang and Z. Wang, J. Colloid Interf. Sci. 2001, 242, 288.

Graphical abstract